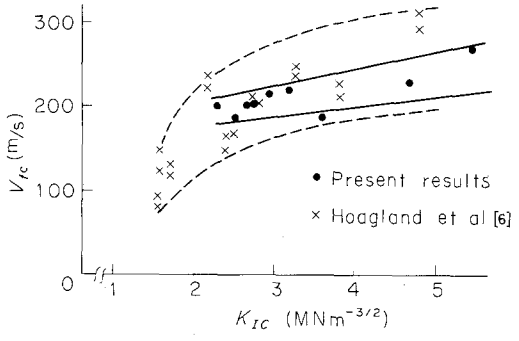

Figure 3 A comparison of K_{IC}–v_{fc} relationships.

et al. used the resistance grid method [1] to measure v_f. Fig. 3 shows that the amount of scatter in plotted values can be reduced by using the ultrasonic fractography method. Experimental details and further fracture mechanics study of propagating cracks in connection with ultrasonic fractography will be published elsewhere.

Acknowledgement

The authors wish to thank S. Yoshino, Y. Mitsui, Y. Nagai and Y. Miyauchi for their help during the course of this work.

References

1. S. R. ANTHONY, J. P. CHUBB and J. CONGLETON, *Phil. Mag.* **22** (1970) 1201.
2. D. PERETZ and A. T. DiBENEDETTO, *Eng. Fract. Mech.* **4** (1972) 979.
3. F. KERKHOF, Naturwiss. **40** (1953) 478.
4. *Idem*, Proceedings of the 3rd International Congress on High-Speed Photography (Butterworths, London, 1956) p. 194.
5. J. H. GREENWOOD, *Int. J. Fract. Mech.* 8 (1972) 183.
6. R. G. HOAGLAND, M. F. KANNINEN, A. J. MARKWORTH, P. N. MINCER and A. R. ROSENFIELD, *Int. J. Fract. Mech.* 8 (1972) 337.
7. W. F. BROWN Jr and J. E. SRAWLEY, STP 410 (ASTM, Philadelphia, 1967).

Received 31 January
and accepted 18 April 1978.

K. TAKAHASHI*
M. KIMURA
S. HYODO
Department of Applied Physics,
The University of Tokyo,
Tokyo,
113 Japan

* Present address: Research Institute for Applied Mechanics, Kyushu University, Hakozaki, Fukuoka, 812 Japan.

Increased fracture toughness of brittle materials by microcracking in an energy dissipative zone at the crack tip

The influence of microcracking on the fracture toughness of brittle materials, especially of ceramics, has been discussed recently in the literature [1–5]. In our paper we shall deal theoretically with the question of under which conditions microcracking would result in an increase of toughness. Our theory is based on experimental results presented by Claussen *et al.* [6, 7]. They examined composites fabricated from Al_2O_3 and unstabilized ZrO_2 powder. The fracture toughness of these composites has a significant maximum in dependence on the volume fraction of ZrO_2 particles. In the optimum case the toughness can be increased by a factor between 2 and 3 in comparison to that of the Al_2O_3 matrix. It is hypothesized by Claussen [7] that this increase results from small matrix microcracks absorbing energy by controlled propagation.

The first attempt to explain theoretically this toughning phenomenon was made by Buresch [8, 9]. In his papers, however, an effective fracture criterion similar to the Dugdale–Barenblatt criterion is used. That is a problematic approach because that criterion presupposes homogeneous stresses within the microcrack zone near the crack tip, which precludes taking into account the direct interaction of the main crack with microcracks.

In our paper another approach will be used. We shall set up a more detailed energy balance of increasing and decreasing effects of microcracks on fracture toughness. Energy variations methods will be used, because they enable us to avoid a detailed calculation of stress and strain distributions. The theoretical model may be explained by Fig. 1, where the tip of a two-dimensional plane crack in an infinite body is shown. When the material is loaded, microcracking occurs in a certain region in the vicinity of the crack tip. The characteristic length of this region, say r_D, depends on the applied load; it will be determined

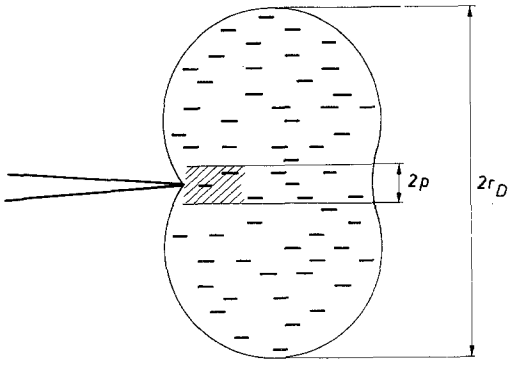

Figure 1 Main crack tip showing "dissipation zone" and "process zone".

later. The microcrack zone is termed by some authors [6, 8] as the "process zone". It seems more appropriate to call it the "dissipation zone", since energy is dissipated within that zone by microcracking. In this paper the term "process zone" denotes the region ahead of the crack tip, where coalescence with microcracks occurs while the main crack is extending. The width of this process zone is denoted by $2p$ (cf. Fig. 1). We shall presuppose the microcracks to be much smaller than the main crack.

The aim of our paper is to calculate the fracture toughness of the material, which is equivalent to the critical energy release rate connected with crack extension. To this end let us consider a small variation $\mathrm{d}l$ of the length of the main crack. The variation should comprise the stochastic coalescence of the main crack with some microcracks within the process zone. The energy per unit thickness required for this variation of crack length is composed of two parts. In the process zone an amount $2\gamma_{\mathrm{eff}}\mathrm{d}l$ is consumed by the formation of new fracture surface (the effective surface energy is smaller than the real surface energy γ of the material owing to coalescence with microcracks). In addition to this, energy is dissipated by the formation and growing of microcracks, because the dissipation zone in Fig. 1 is also shifted by an amount of $\mathrm{d}l$. This energy may be expressed by $\eta 2r_{\mathrm{D}}\,\mathrm{d}l$, where η denotes the dissipated energy per volume and $2r_{\mathrm{D}}\,\mathrm{d}l$ is the newly created area of the dissipation zone in the cross-section of Fig. 1 (the variation of r_{D} is of higher order and may be neglected, which is analogous to the case of "small scale yielding" in ductile fracture mechanics).

Crack extension is possible if the required energy is balanced by the available energy. The latter arises from work of external forces and from release of strain energy of the material and is given by the loss $-\mathrm{d}P$ of potential energy of the system. Since we consider the case of a small dissipation zone, the variation of potential energy is expressible by the critical energy release rate G_{c}, i.e. the fracture toughness:

$$-\mathrm{d}P = G_{\mathrm{c}}\,\mathrm{d}l.$$

Hence we are able to set up the balance of energy

$$-\frac{\mathrm{d}P}{\mathrm{d}l} = G_{\mathrm{c}} = 2\gamma_{\mathrm{eff}} + 2\eta r_{\mathrm{D}} \qquad (1)$$

In the literature one may find different results for r_{D} (e.g. [5, 10]), depending on the shape of the zone, but the common feature of all the solutions is that r_{D} is proportional to $G_{\mathrm{c}}E/\sigma_{\mathrm{c}}^2$, where E is Young's modulus of the material, and σ_{c} the critical maximum stress at which microcracking starts. As mentioned above the factor of proportionality may differ. In our paper we have chosen the value 1/3:

$$r_{\mathrm{D}} = \frac{1}{3}\,\frac{G_{\mathrm{c}}E}{\sigma_{\mathrm{c}}^2} \qquad (2)$$

It is obvious that η, the dissipated energy per volume, must be proportional to $\sigma_{\mathrm{c}}^2/2E$, the stored elastic energy before microcracking occurs

$$\eta = g\,\frac{\sigma_{\mathrm{c}}^2}{2E} \qquad (3)$$

The dissipated energy may be greater or less than the stored energy, because the surrounding area may feed energy into the dissipative zone. Therefore, g is a dimensionless constant depending on some properties of the microcrack array. It will be determined later on.

From Equation 1 to 3 the fracture toughness G_{c} may be derived as

$$\frac{G_{\mathrm{c}}}{2\gamma} = \frac{\gamma_{\mathrm{eff}}/\gamma}{1 - \frac{1}{3}g} \qquad (4)$$

In this equation G_{c} has been normalized by 2γ, which is the fracture toughness of the material without microcracks. The numerator on the right-hand side describes the reduction of toughness by coalescence of the main crack with microcracks,

whereas the denominator represents the additional dissipation of energy by growing microcracks.

In order to determine the quantities γ_{eff}/γ and g in Equation 4, a special model is used. For details of the calculations the reader is referred to [11]. We describe the two-dimensional random array of microcracks by a density:

$$\rho = N/A \cdot (2a)^2. \quad (5)$$

Here N is the number of cracks situated in an area A of the cross-section in Fig. 1. $2a$ is the final length of microcracks (it is a necessary assumption that the created microcracks are stopped at some obstacle, e.g. at grain boundaries). The microcracks are assumed to be oriented parallel to the main crack.

For calculating the dissipated energy η (Equation 3), the microcrack array is considered as a continuum with effective Youngs modulus E^* perpendicular to the crack plane. The function g (Equation 3) is then expressible by the ratio E^*/E:

$$g = g\left(\frac{E^*}{E}\right) = 3\,\frac{1-E^*/E}{1+2E^*/E} \quad (6)$$

The dependence of E^* on the density of microcracks may be derived by means of the "self-consistent scheme" as recently applied by Budiansky [12] to another crack problem. The result reads in our case:

$$\frac{E^*}{E} = 1-\frac{\pi}{2}\rho \quad (7)$$

A geometrical consideration of stochastical coalescence between main crack and microcracks yields the following approximate result for the effective surface energy:

$$\frac{\gamma_{eff}}{\gamma} = 1-\left(\frac{p}{a}\right)\frac{\rho}{(1-\rho\pi/2)^{1/2}} \quad (8)$$

Here the width of the process zone p plays an important role. In more detailed models, additional geometrical parameters may appear in this expression.

With the aid of Equations 4 to 8 the dependence of fracture toughness on the density ρ of created microcracks may be computed. Numerical results are shown in Fig. 2. The parameter p/a, the ratio of width of the process zone to size of microcracks, may be considered to be a property of the material, because it is related to the fracture toughness of the material perpendicular to the crack plane.

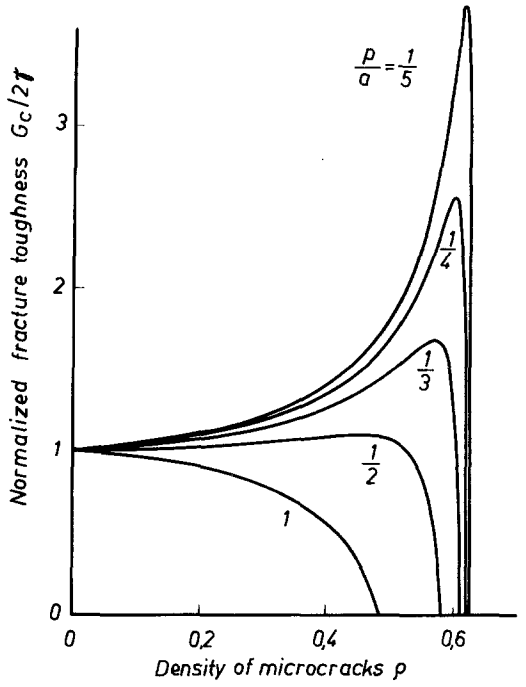

Figure 2 Normalized fracture toughness G_c as a function of microcrack density

By comparing the theoretical predictions with experimental results by Claussen *et al.* [6, 7], their correspondence becomes evident. The theoretical calculations demonstrate the important fact that the generation of stable microcracks is not necessarily connected with an increase in fracture toughness. An increase has to be expected only for special kinds of interaction of these microcracks with the main crack. A small process zone (small p/a) is a condition for this to happen. Such a situation may be found in materials with a laminated structure, e.g. graphite (cf. [9]) and in the case of oriented microcrack nucleation. Also in materials with a micro-duplex structure the range of interaction between microcracks and the main crack may be diminished. Composite materials with ductile and brittle components as well as brittle composites with suitable residual stress distributions are examples of such kinds of materials [13].

References

1. A. G. EVANS, *Scripta Met.* **10** (1976) 93.
2. A. G. EVANS, A. H. HEUER and D. L. PORTER, "Fracture", 1977 Vol. 1 (ICF4, Waterloo, 1977).

3. D. L. PORTER and A. H. HEUER, *J. Amer. Ceram. Soc.* 60 (1977) 183.
4. R. W. RICE, *ibid.* 60 (1977) 280.
5. R. G. HOAGLAND, J. D. EMBURY and D. J. GREEN, *Scripta Met.* 9 (1975) 907.
6. N. CLAUSSEN, *J. Amer. Ceram. Soc.* 59 (1976) 49.
7. N. CLAUSSEN and J. STEEB, *J. Mater. Technol.* 7 (1976) 350.
8. F. E. BURESCH, "Fracture 1977", Vol. 2 (ICF4, Waterloo, 1977).
9. *Idem,* to be published in "Fracture Mechanics of Ceramics" (Proceedings of a symposium held at Pennsylvania State University, July 1977).
10. J. R. RICE, "Fracture", Vol. II, edited by H. Liebowitz (Academic Press, New York and London, 1968).
11. W. KREHER, G. GILLE and W. POMPE, Report ZFW 71 – 77 – 0801, presented at Euromech Colloquium 91, Jablonna, Poland, August 1977.
12. B. BUDIANSKY and R. J. O'CONNELL, *Int. J. Sol. Structures* 12 (1976) 81.
13. N. CLAUSSEN and J. STEEB, *J. Amer. Ceram. Soc.* 59 (1976) 457.

Received 28 February
and accepted 28 April 1978.

W.POMPE
H.-A. BAHR
G. GILLE
W. KREHER
Zentralinstitut für Festkörperphysik und Werkstofforschung der Akademie der Wissenschaften der DDR, Dresden, GDR

The determination of the lattice parameter for $GdCo_2$

In this paper we describe the result of the X-ray analyses of specimens of the cubic Laves phase compounds $GdCo_2$ which were manufactured for pulsed nuclear magnetic resonance investigations of the hyperfine field acting on cobalt nuclei. The specimens were manufactured using an electron beam furnace. Both stoichiometric and non-stoichiometric proportions of gadolinium and cobalt were used in the fabrication of the specimens. Originally non-stoichiometric proportions were used because it was thought than an excess (5 to 15%) of gadolinium would compensate somewhat for the loss of gadolinium from the mixture during the melting process, the gadolinium having a much higher vapour pressure than cobalt at that temperature. However, in the pulsed NMR experiments, and in the X-ray analyses described in this paper, there was no detectable difference between the stoichiometric and the non-stoichiometric specimens. The specimens were formed from an intimate mixture of 4N purity gadolinium powder and 5N purity cobalt powder which were pressed firmly in an extrusion press to form a pellet of 10 mm diameter. This was then placed on the water-cooled hearth of a G.D. Planer electron beam furnace and the furnace was evacuated to a pressure of less than 10^{-6} Torr. The electron beam was than focused on the pellet to melt the specimen. After a temperature of 1100 K was reached the electron beam was turned off and the specimen cooled quickly to room temperature. The melted button was then turned over and remelted several times to ensure that a homogeneous sample was prepared. After manufacture the buttons were filed under alchohol using a diamond hone. Some of the resulting powder specimens were wrapped in tantalum foil and vacuum annealed for 96 h at 1000 K. Others were analysed without annealing.

The X-ray analysis was made using two separate X-ray systems. One comprised a Rigaku SG-7 horizontal goniometer, a Rigaku D9C generator fitted with a fine-focus chromium X-ray tube, and a Xenon proportional detector coupled to a standard Rigaku circuit panel. The second system consisted of a mains stabilized Philips PW1120 generator fitted with a fine focus molybdenum tube. The sample was mounted in a Rigaku 2122B3 vertical gonimeter and the scattered radiation was detected with a Xenon proportional detector coupled to an Ortec counting system. Because the positions of the Bragg reflections had to be known very accurately the diffractometers were calibrated each day using both a silicon powder specimen and a bulk aluminium specimen. Both step-scan and continuous rotation measurements were made. Scans were made in both the clockwise and the anti-clockwise directions.

In an earlier paper [1] it was shown that, for a related Laves phase compound $GdFe_2$, the Bragg reflections were shifted from their expected positions because of deformation faulting. A similar effect is observed for $GdCo_2$ specimens.